

Effects of the presence of Cs impurities on the two-dimensional ^4He phase diagram

M. C. Gordillo and D. M. Ceperley

*National Center for Supercomputing Applications and Department of Physics, University of Illinois at Urbana-Champaign,
405 North Mathews Avenue, Urbana, Illinois 61801*

(Received 26 August 1998)

The changes in the two-dimensional (2D) ^4He phase diagram due to the introduction of impurities (Cs atoms) are estimated using path-integral Monte Carlo simulations. Our results indicate that when we increase the concentration of Cs atoms, the liquid-gas coexistence zone decreases in size and eventually disappears for $\sigma_{\text{Cs}} \sim 0.005 \text{ \AA}^{-2}$, so that 2D ^4He gases will be stable at low temperatures. [S0163-1829(99)03913-2]

There are many studies on the phase diagram of ^4He films adsorbed on various substrates.¹⁻¹⁰ The picture that emerges is that the two-dimensional (2D) fluid separates into a pure 2D liquid and a gas at low temperatures and coverages. In between those two stable phases, there is a sizable coexistence region. The position of the critical point and of the coexistence region are relatively independent of the particular substrate used. In this paper, we raise the question of whether the liquid-gas transition is inevitable, or whether one can find a substrate which is characterized by only a single fluid phase. If so, one would have the possibility of realizing a very low density 2D superfluid, analogous to Bose condensation in atom traps or ^4He in vycor. One cannot have superfluid gases for systems which have a liquid-gas critical point because the maximum density of the gas decreases exponentially with temperature [$\sigma \propto \exp(-e_B/KT)$ with e_B the binding energy of the liquid], so that the conditions needed for the Kosterlitz-Thouless transition temperature ($T_{\text{KT}} \propto \sigma$) cannot be met.

In this paper, we report the results using the path integral Monte Carlo (PIMC) method, of a purely 2D ^4He film on a surface with a finite density of Cs impurities ($0.003 \text{ \AA}^{-2} < \sigma_{\text{Cs}} < 0.012 \text{ \AA}^{-2}$). The ^4He coverage was in the range $0.0 < \sigma_{\text{He}} < 0.06 \text{ \AA}^{-2}$, approximately where the liquid-gas coexistence region is known experimentally to be. This is also the region in which the influence of the substrate is weaker and the helium film is more accurately described by a 2D model.⁹ Since the interaction between helium atoms and alkali metal atoms is primarily repulsive, the binding of helium to the metal is very weak. By changing the number of alkali metal atoms, one can vary the effect of this repulsion and change the ^4He phase diagram. Our calculations predict that impurities reduce the critical temperature of the liquid-gas phase transition. With enough impurities, the critical point disappears altogether, allowing the possibility of a very low density 2D super gas.

The PIMC method allows one to make reliable estimates of the pressure and energy from an assumed interaction potential, thus mapping out the phase diagram. Practical details are given elsewhere.¹² The Cs-He interaction was modeled by a 12:6 Lennard-Jones potential. We deduced the values of σ and ϵ from Ref. 13. $\sigma = 3.8 \text{ \AA}$ was taken so that the minimum of the potential is the average of the atomic radii of the two species and $\epsilon = 0.9 \text{ K}$ was determined by the potential felt by a He atom on a Cs surface. For the He-He interaction

we used the Aziz potential.¹⁴ In any case, the results are insensitive to these values. Note that the model is strictly two-dimensional. The simulation cell was the same as used in Ref. 11: a $17.32 \times 20.0 \text{ \AA}^{-2}$ rectangle, in which we located 1, 2, or 4 Cs impurities. That implies cesium concentrations of 0.003, 0.006, and 0.012 \AA^{-2} . We also used a cell with a smaller area (230 \AA^{-2}) with only one Cs atom ($\sigma_{\text{Cs}} = 0.0043 \text{ \AA}^{-2}$).

To establish the boundaries of the liquid-gas coexistence zone, we looked at the behavior of the pressure as a function of coverage at different temperatures. In a homogeneous system, the pressure must be a monotonically increasing with coverage along an isotherm. On the contrary, if $(dp/d\sigma) < 0$, then there is instability to phase separation. The limit between these two behaviors (the critical temperature) is marked by a flat isotherm. Figure 1 shows the change in the isotherms at $T = 0.25 \text{ K}$ when we increase the number of impurities from 0 (diamonds, Ref. 15), to 1 (crosses), 2 (pluses), and 4 (squares). We see that when we have one impurity or less, the coverage dependence of pressure indicates the presence of a coexistence region. The zero-pressure liquid coverage changes from $\sigma_{\text{He}} = 0.044 \text{ \AA}^{-2}$ for the pure helium case to $\sigma_{\text{He}} = 0.029 \text{ \AA}^{-2}$ when $\sigma_{\text{Cs}} = 0.003 \text{ \AA}^{-2}$.

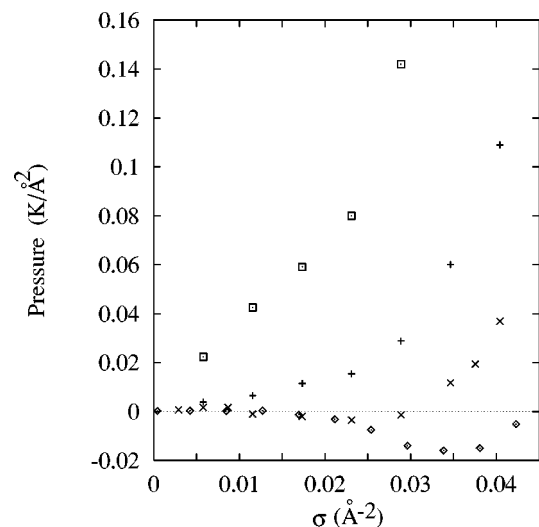


FIG. 1. Calculated pressure versus He (σ) and Cs coverages at $T = 0.25 \text{ K}$: pure helium, \diamond ; $\sigma_{\text{Cs}} = 0.003 \text{ \AA}^{-2}$, \times ; $\sigma_{\text{Cs}} = 0.006 \text{ \AA}^{-2}$, $+$; $\sigma_{\text{Cs}} = 0.012 \text{ \AA}^{-2}$, squares.

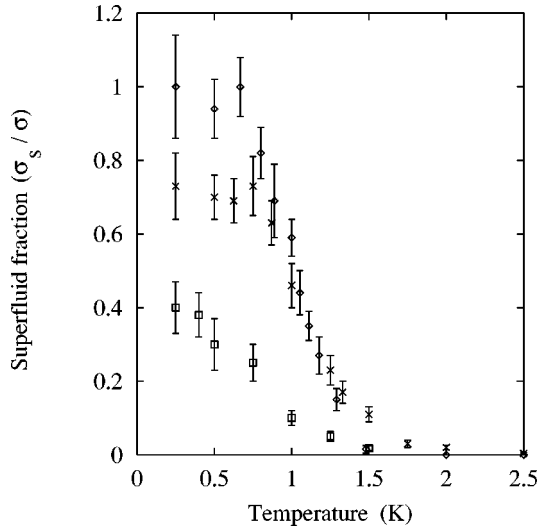


FIG. 2. Superfluid fraction versus temperature. Symbols as in Fig. 1.

On the other hand, when we increase the number of impurities (for the same size of the simulation cell) from 1 to 2 ($\sigma_{\text{Cs}}=0.003 \text{ \AA}^{-2}$), the behavior of the pressure isotherms changes considerably, e.g., at $T=0.25 \text{ K}$ the pressure is monotonically increasing with helium coverage, indicating a lack of phase separation. If we repeat the calculations for $T=0.125 \text{ K}$, we obtain virtually the same values of the pressure, hence we are close to the ground state. This is similar to what happens when the concentration of impurities is 0.012 \AA^{-2} ; the only difference is that the values of the pressure increase even further. We conclude that the liquid-gas coexistence zone disappears and the ground state of a 2D ^4He film is not a self-bound liquid. Such a state will have a flat isotherm when $T \rightarrow 0$. With the help of additional simulations (including one Cs impurity in the 230 \AA^{-2} cell), we estimate that the liquid-gas critical temperature disappears when the Cs concentration is in the range $0.0043 < \sigma < 0.006 \text{ \AA}^{-2}$.

The presence of impurities also affects the superfluid density. Figure 2 shows the temperature dependence of the superfluid fraction $\sigma_s/\sigma_{\text{He}}$ as a function of temperature for three systems with different Cs coverages. The superfluid density σ_s is proportional to the mean-square winding number;¹² winding paths are those that wrap around the periodic boundary conditions. When there are no external obstacles (impurities) to the formation of the winding paths, all atoms eventually contribute to the superfluid fraction¹⁶ at low enough temperatures. However, the introduction of only one impurity in the simulation cell makes $\sim 29\%$ of the He atoms respond to perturbation normally. That number increases up to $\sim 60\%$ for four impurities per cell. That concentration of impurities was used in Ref. 11 to obtain superfluid molecular hydrogen. The He coverage is also very similar to the H_2 coverage used in that work ($\sigma_{\text{H}_2}=0.038 \text{ \AA}^{-2}$), and the dependence of the superfluid fraction on the temperature is virtually identical. This suggests that the superfluid density is primarily determined by the geometry of the system, not by the interaction between particles (providing we have a fluid). There is another effect of impurities on the superfluid film, namely that there exist other

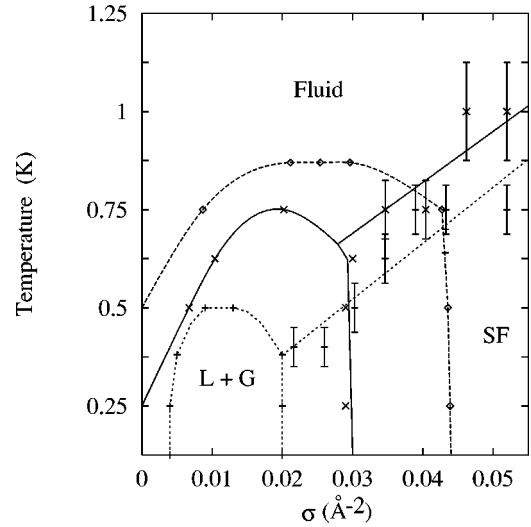


FIG. 3. Phase versus temperature and helium (σ) and Cs coverage: diamonds and dashed line, pure helium system (Ref. 15); crosses and solid line, $\sigma_{\text{Cs}}=0.003 \text{ \AA}^{-2}$; pluses and dotted line, $\sigma_{\text{Cs}}=0.0043 \text{ \AA}^{-2}$.

topological quantities besides the winding number, such as the phase picked up by the wave function as an atom encircles an impurity. It would be of interest to calculate the mean-square value of these phases in equilibrium with path integrals.

As we mentioned above, when $\sigma_{\text{Cs}} < 0.006 \text{ \AA}^{-2}$, some of the isotherms have a coverage range in which $(dp/d\sigma) < 0$, indicating a two-phase coexistence. We determined the limits of this region by matching the chemical potentials of the two phases involved, i.e.,

$$\int_{A_G}^{A_L} p dA = \int_{\sigma_G}^{\sigma_L} \frac{\sigma_L - p}{\sigma^2} d\sigma = 0, \quad (1)$$

where σ_G and σ_L are the equilibrium coverages of the gas and liquid phases, respectively. The integrals were performed by fitting the pressure to a polynomial in temperature. The boundaries of those regions are displayed in Fig. 3. The solid line represents the limits when $\sigma_{\text{Cs}}=0.003 \text{ \AA}^{-2}$, and the dotted line those same boundaries when $\sigma_{\text{Cs}}=0.0043 \text{ \AA}^{-2}$. The dashed line indicates the data for the pure system.¹⁵ In agreement with the above discussion, we observe that the area of the two-phase region shrinks as the impurity concentration increases and the liquid-gas critical temperature decreases: $T_c=0.75 \text{ K}$ in the first case, and 0.38 K in the second, versus 0.87 K (Ref. 15) for the pure system. We observe also that for $\sigma_{\text{Cs}}=0.0043 \text{ \AA}^{-2}$, there is a low-temperature stable gas phase.

The two diagonal lines at the right part of the figure are the limits of the superfluid region. They are defined by fitting the simulation results for each impurity concentration (symbols) to two straight lines. The boundary in the pure case, not shown here for simplicity, lies in between the two lines.¹⁵ The critical temperatures is determined by the edge of the plateau in the superfluid density versus temperature (e.g., Fig. 2). We have not performed a detailed finite-size analysis, nevertheless, this is a good estimate of when the Kosterlitz-Thouless transition will occur.

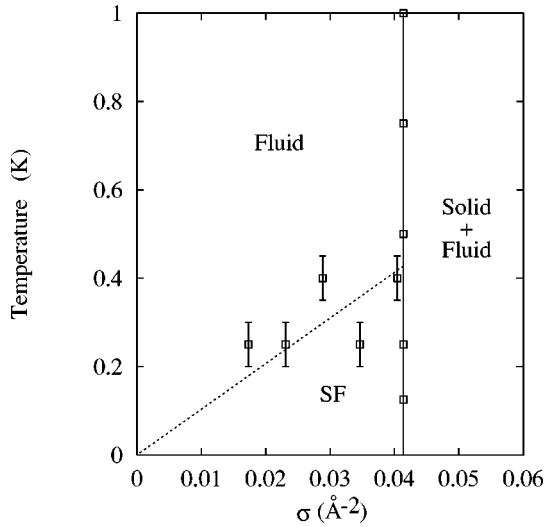


FIG. 4. Same as in Fig. 3 with $\sigma_{Cs}=0.012 \text{ \AA}^{-2}$.

There have been suggestions that if the liquid-gas critical temperature is decreased enough and a low density phase becomes stable, this phase could be a second superfluid,¹⁷ in equilibrium with the liquid superfluid. However, our results do not show superfluid coexistence, at least for the impurity concentrations presented here. The lowering of the liquid-gas critical temperature is accompanied by a lowering of the line of critical temperature for the superfluid transition. However, since when we further increase the concentration of impurities (see below) we get a superfluid gas with no liquid-gas coexistence zone, it is not inconceivable that there will be such a low density coexisting superfluid phase for some value of impurity concentration.

Figure 4 shows the phase diagram when $\sigma_{Cs}=0.012 \text{ \AA}^{-2}$. As shown in Fig. 1 the pressure is a monotonically increasing function of the coverage for low temperatures. The energies and pressures at 0.25 and 0.125 K are virtually identical, indicating that the system is in the ground state with no sign of phase separation. The fact that the system is a gas is also supported by the energy shown in Fig. 5:

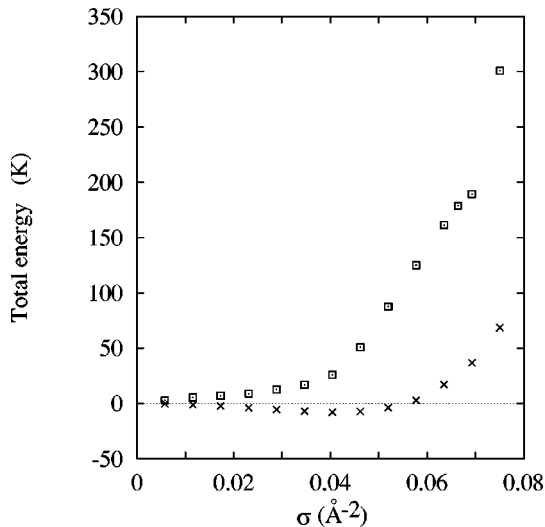


FIG. 5. Total energy per simulation cell versus helium coverage at $T=0.25 \text{ K}$: \times , $\sigma_{Cs}=0.003 \text{ \AA}^{-2}$; squares, $\sigma_{Cs}=0.012 \text{ \AA}^{-2}$.

the kinetic energy is greater than the potential one, and the total energy is positive.

As the helium coverage is increased at fixed density, a localized phase occurs. In the PIMC simulation, we observe this phase by a dramatic change in the structure factor from a smooth curve to a function with large peaks. We performed a Maxwell construction (see Fig. 5) to obtain the limits of the ‘‘solid’’-fluid coexistence region obtaining 0.042 and 0.069 \AA^{-2} . The densities do not change appreciably over the temperature interval shown. We used the energy in the Maxwell construction because the entropy term in the free energy is not important, for temperatures less than 1 K .

The symbols with error bars in the fluid part of the phase diagram are our estimates of the superfluid-normal fluid phase transition temperature obtained as in Fig. 3: they represent the temperature at which the superfluid density flattens out. For He concentrations below 0.015 \AA^{-2} , we do not observe a nonzero superfluid density, possibly due to inadequate convergence of the PIMC calculation. The dotted line represents a fit of the data for the five concentrations from which we can obtain a value for T_c . The fit was forced to pass through the origin.

In principle, a bosonic system could have a gas (not a condensed liquid) ground state providing that its de Boer parameter ($\hbar^2/m\epsilon_{LJ}\sigma_{LJ}^2$) is large enough.¹⁸ We think that we have fulfilled that condition because the effective attraction between helium atoms is lowered by the Cs impurities. To verify this, we performed an additional series of simulations using a single Xe atom as a impurity in the same simulation cell employed above. We found that, for a given temperature, the pressure decreases in relation to the values of the pure He case, i.e., the size of the liquid-gas coexistence zone increases instead of disappearing.

Another way of decreasing the de Boer parameter is to keep the interparticle interaction constant but reduce the density of the system by diluting with ^3He . In that case, one would expect a similar behavior to what we see with Cs impurities. In fact, the experimental data of Ramos, Ebey,

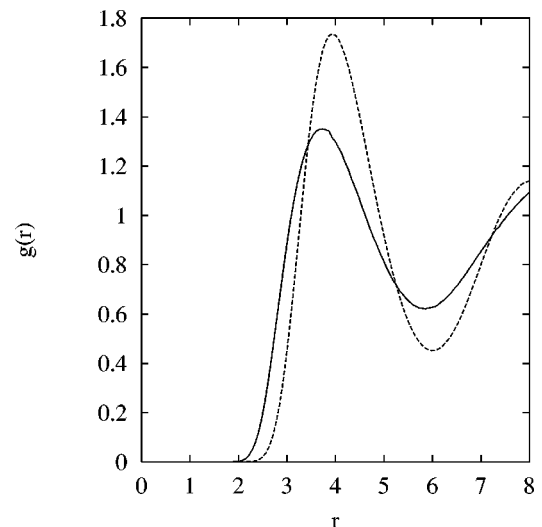


FIG. 6. The pair-correlation function for He (solid line) and H_2 (Ref. 11) (dashed line). Both systems are at a coverage $\sigma=0.04 \text{ \AA}^{-2}$, $T=1 \text{ K}$ and with the same Cs coverage: $\sigma_{Cs}=0.01 \text{ \AA}^{-2}$.

and Vilches⁵ show such an effect. They observe a significant lowering of the critical temperature of the liquid-gas transition as the molar fraction of ³He increases. Their results also indicate that they would need a much larger concentration of ³He than Cs to reduce the critical temperature by the same amount.

That leaves us with the problem of finding an adequate substrate to observe these effects. We modeled the cell with 4 Cs atoms after a low-temperature phase found in Rb and Cs atoms adsorbed on Ag(111).¹⁹ Any substrate, even a non-metallic one, where the alkali metal atoms are not ionized and are uniformly spread on the surface should have the effect of reducing the liquid density. We think our 2D model captures the important effects of such a system.¹¹ In Ag(111) the lowest experimental coverage tried was about 0.008 \AA^{-2} for Cs,²⁰ but there could be less dense phases, allowing one experimentally to approach the concentration at which the liquid-gas critical point disappears.

Recent calculations on a 2D film of H₂ (Ref. 11) indicate that K and Cs impurities on a smooth metal surface will stabilize a liquid phase of H₂ at low temperatures and prevent the solidification characteristic of a clean layer of H₂. Hence, the fluid becomes superfluid below 1 K. In Fig. 6 we compare the radial distribution functions of the fluid He and H₂. Both functions are characteristic of a strongly correlated quantum fluid, but it is seen that H₂ is more strongly correlated, due to the larger size and intermolecular interaction of H₂. Because of the stronger attraction, it is not likely that H₂ will have a low density super-gas phase.

ACKNOWLEDGMENTS

This research was supported by NSF Grant No. DMR 94-224-96 and the Department of Physics of the University of Illinois at Urbana-Champaign and computational facilities at the NCSA.

-
- ¹S.E. Polanco and M. Bretz, Phys. Rev. B **17**, 151 (1978).
²D.S. Greywall and P.A. Busch, Phys. Rev. Lett. **67**, 3535 (1991).
³D.S. Greywall, Phys. Rev. B **47**, 309 (1993).
⁴P.S. Ebey and O.E. Vilches, J. Low Temp. Phys. **101**, 469 (1995).
⁵R.C. Ramos, Jr., P.S. Ebey, and O.E. Vilches, J. Low Temp. Phys. **110**, 615 (1998).
⁶D.J. Bishop, J.E. Berthold, J.M. Parpia, and J.D. Reppy, Phys. Rev. B **24**, 5047 (1981).
⁷P.A. Crowell and J.D. Reppy, Phys. Rev. Lett. **70**, 3291 (1993).
⁸P.A. Crowell and J.D. Reppy, Physica B **197**, 269 (1994).
⁹P.A. Crowell and J.D. Reppy, Phys. Rev. B **53**, 2701 (1996).
¹⁰J. Nyèki, R. Ray, V. Moidanov, M. Siqueira, B. Cowan, and J. Saunders, J. Low Temp. Phys. **101**, 279 (1995).
¹¹M.C. Gordillo and D.M. Ceperley, Phys. Rev. Lett. **79**, 3010 (1997).
¹²D.M. Ceperley, Rev. Mod. Phys. **67**, 279 (1995).
¹³E. Cheng, M.W. Cole, W.F. Saam, and J. Treiner, Phys. Rev. B **46**, 13 967 (1992).
¹⁴R.A. Aziz, A.R. Janzen, and M.R. Moldover, Phys. Rev. Lett. **74**, 1586 (1995).
¹⁵M.C. Gordillo and D.M. Ceperley, Phys. Rev. B **58**, 6447 (1998).
¹⁶D.M. Ceperley and E.L. Pollock, Phys. Rev. B **39**, 2084 (1989).
¹⁷M. Schick and O.E. Vilches, Phys. Rev. B **48**, 9910 (1993).
¹⁸L.H. Nosanow, J. Phys. (Paris), Colloq. **41**, C7-1 (1980).
¹⁹G.S. Leatherman and R.D. Diehl, Phys. Rev. B **53**, 4939 (1996).
²⁰R.D. Diehl and R. McGrath, Surf. Sci. Rep. **23**, 43 (1996).